

Chiral $\mathcal{O}(Q^4)$ two-body operators for s -wave pion photoproduction on the NN system

A. Gårdestig*

*Department of Physics and Astronomy,
University of South Carolina, Columbia, SC 29208*

(Dated: August 10, 2018)

Abstract

The two-body currents for s -wave pion photoproduction on the NN system are derived to $\mathcal{O}(Q^4)$ in chiral perturbation theory. For the interesting case of ${}^3S_1 \leftrightarrow {}^1S_0$ transitions, we show that an axial isovector two-nucleon contact term connects the short-distance physics of pion photoproduction to pion production and several important electroweak reactions. We also find that the standard chiral Lagrangian gives a $\gamma\pi\pi NN$ vertex that have not been explicitly mentioned in previous literature. The corresponding Feynman rule is presented here and some processes where it should be important are briefly discussed.

PACS numbers: 21.45.+v, 12.39.Fe, 13.75.Cs, 25.80.Hp

Keywords: chiral perturbation theory, pion photoproduction

*Electronic address: anders@physics.sc.edu

Photo- and electroproduction of pions on nucleons have been intensely studied in the framework of chiral perturbation theory (χ PT). Calculations exist for $\gamma d \rightarrow \pi^0 d$ [1], $\gamma^* d \rightarrow \pi^0 d$ [2], $\gamma^{(*)} N \rightarrow \pi N$ [3], $\gamma p \rightarrow \pi^0 \pi^0 p$ [4], and $\gamma d \rightarrow nn\pi^+$ [5]. Recently, also radiative pion absorption on the deuteron has been calculated using χ PT [6, 7]. The latter work is motivated by the crucial importance the $\pi^- d \rightarrow nn\gamma$ measurements play for the extraction of the neutron-neutron scattering length (a_{nn}) [8] and the corresponding need for a precise and accurate theoretical calculation.

The advantage of using χ PT (apart from providing a tractable low-energy limit of QCD) is that it is an effective field theory based on an expansion in the ratio $\chi = Q/M_{\text{QCD}}$, where $Q \sim m_\pi$ is the size of typical momenta and energies in the problem (m_π is the pion mass) and $M_{\text{QCD}} = \mathcal{O}(1 \text{ GeV})$ is the energy scale at which this EFT breaks down. In the following, we will assume that $M_{\text{QCD}} \equiv M$ (the nucleon mass) and that the electron charge $e < 0$ also counts as the small scale Q . (A detailed review of χ PT can be found, e.g., in Ref. [9].) This expansion not only provides a prescription on how to estimate errors, but also suggest what needs to be done in order to improve the precision of the calculation.

In this brief note we derive the $\mathcal{O}(Q^4)$ two-body contributions to s -wave pion photoproduction in Coulomb gauge. The amplitudes for neutral pion photoproduction were used in Refs [2], though no expressions were given. We will find that the standard chiral Lagrangian gives an additional $\gamma\pi\pi NN$ vertex that have not been explicitly mentioned in previous literature, though it was included in the calculations of [2, 10]. We derive the corresponding Feynman rule and discuss some reactions where it should be important. We will also explicitly prove that the two-body contact term needed in [7] to reduce the theoretical error in the $\pi^- d \rightarrow nn\gamma$ calculations is indeed the same as the one appearing in weak pp fusion, tritium β decay, the hep process (${}^3\text{He} p \rightarrow {}^4\text{He} e^+ \nu_e$), $\nu(\bar{\nu})d$ breakup, and $\mu^- d \rightarrow nn\nu_\mu$, as well as in p -wave pion production on two nucleons and the chiral three-nucleon force (3NF). This identity can be established only if the additional Feynman rule is included.

The $\pi N(N)$ terms of the chiral Lagrangian relevant for the $\mathcal{O}(Q^4)$ amplitudes are [9, 11]

$$\mathcal{L}_{\pi N}^{(1)} = N^\dagger [i v \cdot D + g_A S \cdot u] N, \quad (1)$$

$$\begin{aligned} \mathcal{L}_{\pi N+\pi NN}^{(2)} = & N^\dagger \left[\frac{v^\mu v^\nu - g^{\mu\nu}}{2M} D_\mu D_\nu + c_3 u \cdot u + \left(c_4 + \frac{1}{4M} \right) [S^\mu, S^\nu] u_\mu u_\nu \right] N \\ & - 2d_1 N^\dagger S \cdot u N N^\dagger N + d_2 \epsilon^{abc} \epsilon_{\kappa\lambda\mu\nu} v^\kappa u^{\lambda,a} N^\dagger S^\mu \tau^b N N^\dagger S^\nu \tau^c N, \end{aligned} \quad (2)$$

where v is the nucleon four-velocity, D is a (chiral) covariant derivative, S is the Pauli-

Lubanski spin vector, and g_A parametrizes the unknown short-distance physics of the nucleon's axial-current matrix element. The low-energy constants (LECs) $c_i = \mathcal{O}(\frac{1}{M})$ parametrize pion rescattering on one nucleon, while the $d_i = \mathcal{O}(\frac{1}{Mf_\pi^2})$ parametrize the two-nucleon axial isovector contact term [19]. The latter have to be determined from fits to suitable two-nucleon data. Here u_μ is an axial four-vector which contains the pion field, and when expanded takes the form:

$$u_\mu = -\frac{\tau^a \partial_\mu \pi^a}{f_\pi} - \frac{\epsilon^{3ba} V_\mu \pi^b \tau^a}{f_\pi} + A_\mu + \mathcal{O}(\pi^3) \quad (3)$$

where V_μ (A_μ) is an external vector (axial) field and $f_\pi = 93$ MeV is the pion decay constant. Note that only the isovector part of the vector field contributes at this order. (u_μ^a is obtained by factoring out τ^a .)

At next-to-leading order [NLO or $\mathcal{O}(Q^4)$] a slew of diagrams appear, given in Fig. 1. These diagrams are the same as the ones in Refs. [1, 2], except that here only diagrams giving s -wave pions are shown. The diagrams have been grouped together according to their pion propagator structure. Thus, the first row [(a)–(d)] have a Coulomb-like propagator since the energy of the photon has to be transferred through the exchanged pion in order to produce a final, real pion, while row two [(e)–(g)] has an off-shell (zero energy transfer) pion propagator, and row three [(i)–(k)] has one propagator of each kind. The initial virtual pion in (e) and (i) is emitted in an s -wave (from $\mathcal{L}_{\pi N + \pi NN}^{(2)}$), which makes these terms proportional to the (in this case) very small energy of this pion. Thus these diagrams are pushed to higher order because of kinematics and will not be considered here. In addition, diagram (e) will vanish in the Coulomb gauge. The stretched pion exchange diagram (l) was included in [1, 2], where it was evaluated in time-ordered perturbation theory, but its evaluation depends on the way the attached wave functions are constructed, e.g., if they are energy-dependent or not. For this reason, we will not derive explicit expressions for this type of diagram. Finally, diagram (m) contains the two-body contact terms given by the LECs d_1 and d_2 . Explicit expressions for the surviving diagrams are given in the Appendix.

In principle, diagrams (c), (d), (f), (g), (h), and (k) should all have contact terms, i.e., they contain constant pieces that gets Fourier transformed into $\delta^{(3)}(\mathbf{r})$ in configuration space. However, for ${}^3S_1 \leftrightarrow {}^1S_0$ transitions the $(\frac{g_A^3}{Mf_\pi^3})$ contributions from (c) and (g) will partially cancel against (k), while the $(\frac{g_A}{Mf_\pi^3})$ contributions from (d) and (h) will be completely canceled by a term from (f). This leaves the contact terms given by c_3 , $c_4 + \frac{1}{4M}$ [from (f)], d_1 , d_2

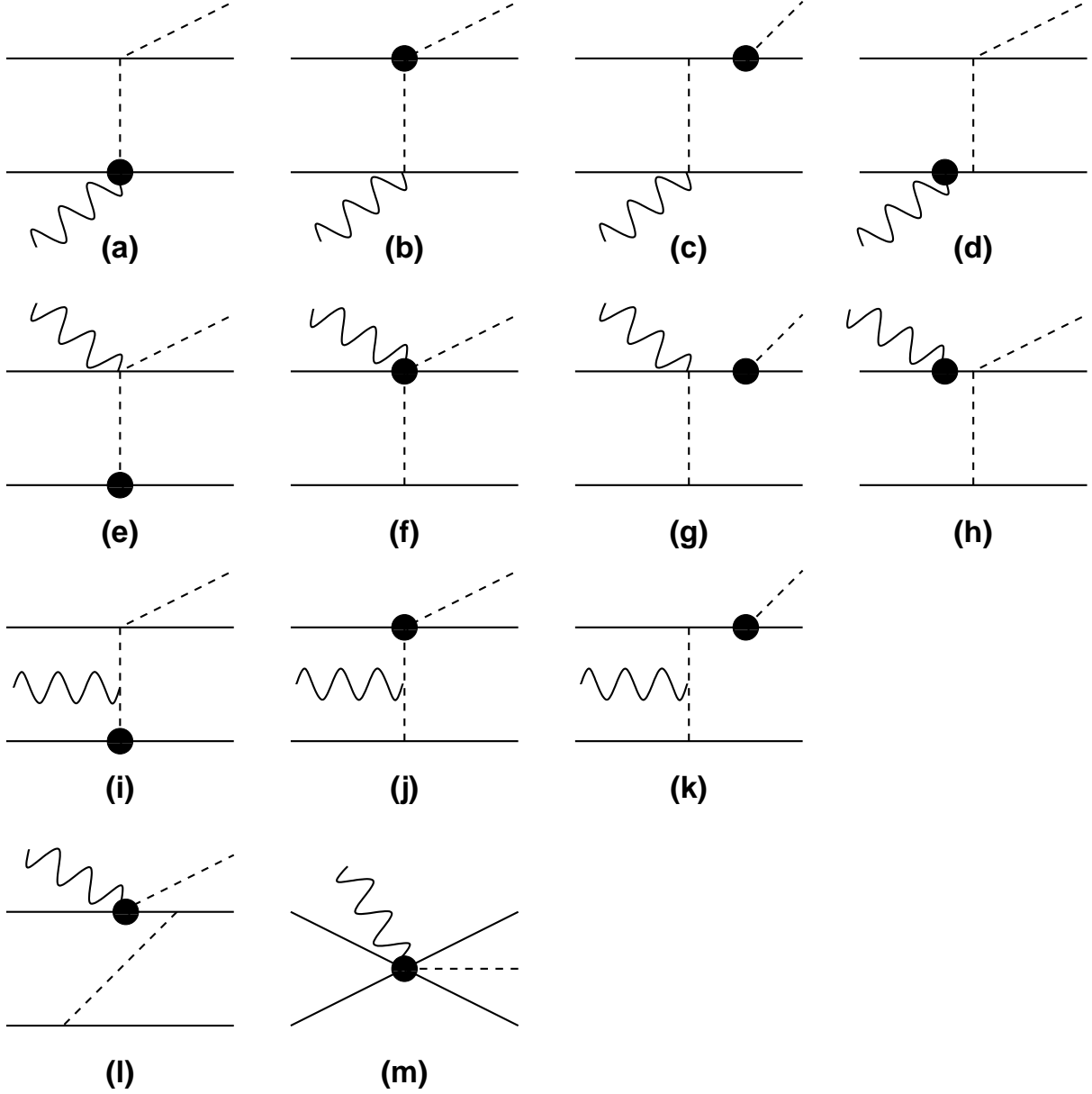


FIG. 1: Next-to-leading-order [$\mathcal{O}(Q^4)$] two-body diagrams for s -wave pion photo-production on two nucleons. Only one representative vertex ordering is given for each type of diagram. The black disc indicates an insertion from $\mathcal{L}_{\pi N + \pi NN}^{(2)}$.

[from (m)], and the surviving g_A^3 piece from (c), (g), and (k) as the only relevant ones. The contact terms linear in g_A will always appear (for ${}^3S_1 \leftrightarrow {}^1S_0$) with the combined coefficient

$$\hat{d} \equiv \hat{d}_1 + 2\hat{d}_2 + \frac{\hat{c}_3}{3} + \frac{2\hat{c}_4}{3} + \frac{1}{6}, \quad (4)$$

as explained in the appendix. The g_A^3 contact term appears only in the $\pi^- d \rightarrow nn\gamma$ and

$\gamma d \rightarrow nn\pi^+$ reactions. The reduced (dimensionless) LECs \hat{c}_i and \hat{d}_i are defined through

$$c_i \equiv \frac{\hat{c}_i}{M}, \quad d_i \equiv \frac{g_A \hat{d}_i}{M f_\pi^2}. \quad (5)$$

As claimed in [7], the expression (4) is the same as the one appearing in pp fusion, tritium β decay, and the hep reaction [11], neutrino-induced deuteron breakup [14], muon capture on deuterium [15], p -wave pion production on two nucleons, and the chiral 3NF [16]. Because of Fermi-Dirac statistics, the LECs \hat{d}_i will always appear in the linear combination $\hat{d}_1 + 2\hat{d}_2$ [11].

The gauged c_4 term [derived from the Lagrangian (2) and part of diagram (f)] has not, to the best of our knowledge, been explicitly mentioned in the literature before, i.e., it is missing in the Feynman rules derived in Ref. [9] [their Eq. (A.31)] [10]. The Feynman rule for this term can be written (in a notation reminiscent of [9]) as

$$\left(c_4 + \frac{1}{4M}\right) \frac{2ie}{f_\pi^2} \left[(\delta^{ab}\tau^3 - \delta^{a3}\tau^b) [S \cdot q_1, S \cdot \epsilon_\gamma] - (\delta^{ab}\tau^3 - \delta^{b3}\tau^a) [S \cdot q_2, S \cdot \epsilon_\gamma] \right], \quad (6)$$

where $a, 1(b, 2)$ annotate the incoming (outgoing) pion's isospin and four-momentum. The corresponding pion rescattering diagram (f) is the only way to obtain the c_4 contribution needed for \hat{d} in $\pi^- d \rightarrow nn\gamma$ or $\gamma d \rightarrow nn\pi^+$. In these ${}^3S_1 \leftrightarrow {}^1S_0$ transitions, the rescattered pion emitted by the gauged c_3 and c_4 terms is in an s -wave relative to the nucleon pair. This should be contrasted with $\gamma^{(*)}d \rightarrow \pi^0 d$, where c_4 (but not c_3) can contribute and gives a p -wave pion only. This c_4 term was included in the $\gamma^* d \rightarrow \pi^0 d$ calculations of Refs. [2, 10], but without being explicitly referred to. It will also contribute to $\mathcal{O}(Q^2)$ (charged) double-pion photoproduction on a single nucleon above threshold.

Explicit expressions for the different surviving diagrams of Fig. 1 are given in the appendix. As mentioned above, there appears an extra contact term from diagrams (c), (g), and (k) that did not appear in the other reactions mentioned. However, it enters with a known coefficient and thus does not destroy the linear correlation between the Gamow-Teller matrix element and the FSI peak height that was used in Ref. [7] to reduce the theoretical error in the extracted a_{nn} . Even so, this term does shift the location of the correlation (it changes the FSI peak height) and is therefore necessary for an accurate extraction of a_{nn} .

In this paper we have derived the $\mathcal{O}(Q^4)$ two-body amplitudes for s -wave radiative pion capture or pion photoproduction on two nucleons. We have also shown that the axial isovector contact term for these processes can be parametrized by the same single constant that is used for certain electroweak reactions (like pp fusion and the hep process), p -wave

pion production on two nucleons, and the chiral three-nucleon force. This was accomplished through deriving an additional, previously not published, Feynman rule (parametrized by c_4) for a photon coupling to two pions and one nucleon. This vertex should play a role in $\pi^-d \rightarrow nn\gamma$ [7, 17] and $\gamma d \rightarrow nn\pi^+$, as well as in $\gamma^{(*)}d \rightarrow \pi^0d$ [2] and $\gamma N \rightarrow \pi\pi N$ beyond threshold, for the latter two reactions resulting in p -wave pions. Depending on selection rules for a particular reaction, recoil corrections might become important [5]. Further work on this may be needed—together with a calculation of $\mathcal{O}(Q^4)$ single-nucleon amplitudes and an investigation of when the time-ordered diagram of Fig. 1(1) needs to be included. This will also necessitate a thorough understanding of how to consistently include $1/M$ corrections in operators and the NN potentials used to derive wave functions. We note that weak axial two-body currents and contact terms have been studied recently, from a somewhat different perspective, by Mosconi, Ricci, and Truhlík [18].

The results presented here are important for the calculation of $\pi^-d \rightarrow nn\gamma$ for two reasons. Firstly, it supports the conclusion of Ref. [7] that there is a correlation between the short-distance physics in electroweak reactions and $\pi^-d \rightarrow nn\gamma$. Secondly, it gives expressions for the long-range $\mathcal{O}(Q^4)$ currents that should give a correction to a_{nn} . These currents, together with consideration of the issues raised in Refs. [5, 18], will be included in forthcoming work on a precision computation of the $\pi^-d \rightarrow nn\gamma$ spectrum [17].

It is a pleasure to acknowledge discussions with Fred Myhrer, Kuniharu Kubodera, and Daniel Phillips. I appreciate communications from Veronique Bernard and Ulf-G. Meißner regarding their use of the Feynman rule presented here. This work was supported in part by the National Science Foundation grant PHY-0457014.

APPENDIX: EXPRESSIONS FOR $\mathcal{O}(Q^4)$ TWO-BODY DIAGRAM

We give here momentum-space expressions for the diagrams of Fig. 1 for the case of s -wave pion photoproduction. These formulas can also be used for $\pi^-d \rightarrow nn\gamma$ by time-reversal invariance. In the equations below, we assume that $\tilde{\mathbf{p}} = \mathbf{p}'' - \mathbf{p}'$ and $2\mathbf{P} = \mathbf{p}'' + \mathbf{p}'$, where $\mathbf{p}'(\mathbf{p}'')$ is the relative momentum of the incoming (outgoing) nucleon pair. Also, $\boldsymbol{\epsilon}_d$ and $\boldsymbol{\epsilon}_\gamma$ are the deuteron and photon polarization vectors, while \mathbf{k} is the photon wave vector and $\kappa_{0(1)}$ is the isoscalar (isovector) anomalous nucleon moment. Everything is expressed in the overall rest frame. When doing the replacement ($1 \leftrightarrow 2$), the momenta $\tilde{\mathbf{p}}$ and \mathbf{P}

change sign. It is assumed that contact term contributions should not be included when evaluating the expressions (A.1)–(A.11) below (i.e., that $\delta^{(3)}(\mathbf{r})$ terms should be dropped when performing the Fourier transform). They are instead given explicitly in Eq. (A.12).

1. Coulombic diagrams

The momentum-space expressions for the first row of diagrams in Fig. 1 are

$$\mathcal{O}_a = \frac{eg_A}{8Mf_\pi^3} \frac{\boldsymbol{\sigma}_1 \cdot \boldsymbol{\epsilon}_\gamma}{\left(\tilde{\mathbf{p}} - \frac{\mathbf{k}}{2}\right)^2} \left(\epsilon^{abc} \tau_1^b \tau_2^c + \epsilon^{a3b} \tau_2^b \right) m_\pi^2 + (1 \leftrightarrow 2), \quad (\text{A.1})$$

$$\begin{aligned} \mathcal{O}_b = & \frac{eg_A}{16Mf_\pi^3} \frac{\boldsymbol{\sigma}_1 \cdot \boldsymbol{\epsilon}_\gamma}{\left(\tilde{\mathbf{p}} - \frac{\mathbf{k}}{2}\right)^2} \left[8\epsilon^{a3b} \tau_1^b \left(4\hat{c}_1 - 2\hat{c}_2 - 2\hat{c}_3 + \frac{g_A^2}{4} \right) m_\pi^2 \right. \\ & \left. - i \left(\delta^{a3} \boldsymbol{\tau}_1 \cdot \boldsymbol{\tau}_2 - \tau_1^a \tau_2^3 \right) \left(2\mathbf{P} + \frac{\mathbf{k}}{2} \right) \cdot \left(\tilde{\mathbf{p}} - \frac{\mathbf{k}}{2} \right) \right] + (1 \leftrightarrow 2), \quad (\text{A.2}) \end{aligned}$$

$$\begin{aligned} \mathcal{O}_c = & \frac{eg_A^3}{8Mf_\pi^3} \frac{\boldsymbol{\sigma}_1 \cdot \boldsymbol{\epsilon}_\gamma}{\left(\tilde{\mathbf{p}} - \frac{\mathbf{k}}{2}\right)^2} \left\{ \epsilon^{a3b} \tau_1^b \left[i\boldsymbol{\sigma}_2 \cdot \left(\tilde{\mathbf{p}} - \frac{\mathbf{k}}{2} \right) \times \left(2\mathbf{P} + \frac{\mathbf{k}}{2} \right) \right] \right. \\ & \left. + i \left(\delta^{a3} \boldsymbol{\tau}_1 \cdot \boldsymbol{\tau}_2 - \tau_1^a \tau_2^3 \right) \left(2\mathbf{P} + \frac{\mathbf{k}}{2} \right) \cdot \left(\tilde{\mathbf{p}} - \frac{\mathbf{k}}{2} \right) \right\} + (1 \leftrightarrow 2), \quad (\text{A.3}) \end{aligned}$$

$$\begin{aligned} \mathcal{O}_d = & \frac{eg_A}{8Mf_\pi^3} \frac{1}{\left(\tilde{\mathbf{p}} - \frac{\mathbf{k}}{2}\right)^2} \left\{ - \left(\epsilon^{abc} \tau_1^b \tau_2^c + \epsilon^{a3b} \tau_2^b \right) \boldsymbol{\sigma}_1 \cdot \left(\tilde{\mathbf{p}} - \frac{\mathbf{k}}{2} \right) \boldsymbol{\epsilon}_\gamma \cdot \tilde{\mathbf{p}} \right. \\ & - \left(\delta^{a3} \boldsymbol{\tau}_1 \cdot \boldsymbol{\tau}_2 - \tau_1^a \tau_2^3 \right) \left[(1 + \kappa_1) \tilde{\mathbf{p}} \cdot (\boldsymbol{\epsilon}_\gamma \times \mathbf{k}) + i\boldsymbol{\sigma}_1 \cdot \left(\tilde{\mathbf{p}} - \frac{\mathbf{k}}{2} \right) \boldsymbol{\epsilon}_\gamma \cdot 2\mathbf{P} \right] \\ & \left. + \left[(1 + \kappa_0) \epsilon^{abc} \tau_1^b \tau_2^c + (1 + \kappa_1) \epsilon^{a3b} \tau_2^b \right] \left[\boldsymbol{\sigma}_1 \cdot \boldsymbol{\epsilon}_\gamma \mathbf{k} \cdot \left(\tilde{\mathbf{p}} - \frac{\mathbf{k}}{2} \right) - \boldsymbol{\sigma}_1 \cdot \mathbf{k} \boldsymbol{\epsilon}_\gamma \cdot \tilde{\mathbf{p}} \right] \right\} \\ & + (1 \leftrightarrow 2). \quad (\text{A.4}) \end{aligned}$$

2. Non-Coulombic diagrams

The momentum-space expressions for the second row of diagrams in Fig. 1 are

$$\mathcal{O}_e = 0, \quad (\text{A.5})$$

$$\begin{aligned} \mathcal{O}_f = & \frac{eg_A}{16Mf_\pi^3} \frac{\boldsymbol{\sigma}_1 \cdot \left(\tilde{\mathbf{p}} + \frac{\mathbf{k}}{2} \right)}{\left(\tilde{\mathbf{p}} + \frac{\mathbf{k}}{2} \right)^2 + m_\pi^2} \left[4 \left(\delta^{a3} \boldsymbol{\tau}_1 \cdot \boldsymbol{\tau}_2 + \tau_1^3 \tau_2^a - 2\tau_1^a \tau_2^3 \right) \right. \\ & \times \left[(1 + \kappa_1) \boldsymbol{\sigma}_2 \cdot (\boldsymbol{\epsilon}_\gamma \times \mathbf{k}) - 2i\boldsymbol{\epsilon}_\gamma \cdot \mathbf{P} \right] \\ & + \left[\epsilon^{abc} \tau_1^b \tau_2^c + (16\hat{c}_3 - 1) \epsilon^{a3b} \tau_1^b \right] \boldsymbol{\epsilon}_\gamma \cdot \tilde{\mathbf{p}} \\ & \left. + 2(4\hat{c}_4 + 1) \left(\tau_1^3 \tau_2^a - \tau_1^a \tau_2^3 \right) \boldsymbol{\sigma}_2 \cdot \left(\tilde{\mathbf{p}} + \frac{\mathbf{k}}{2} \right) \times \boldsymbol{\epsilon}_\gamma \right] + (1 \leftrightarrow 2), \quad (\text{A.6}) \end{aligned}$$

$$\begin{aligned} \mathcal{O}_g = & \frac{eg_A^3}{8Mf_\pi^3} \frac{\boldsymbol{\sigma}_1 \cdot (\tilde{\mathbf{p}} + \frac{\mathbf{k}}{2})}{(\tilde{\mathbf{p}} + \frac{\mathbf{k}}{2})^2 + m_\pi^2} \left\{ -\epsilon^{a3b} \tau_1^b \left[\tilde{\mathbf{p}} \cdot \boldsymbol{\epsilon}_\gamma + i\boldsymbol{\sigma}_2 \cdot \left(2\mathbf{P} + \frac{\mathbf{k}}{2} \right) \times \boldsymbol{\epsilon}_\gamma \right] \right. \\ & \left. + i \left(\delta^{a3} \boldsymbol{\tau}_1 \cdot \boldsymbol{\tau}_2 - \tau_1^a \tau_2^3 \right) \left[2\mathbf{P} \cdot \boldsymbol{\epsilon}_\gamma + i\boldsymbol{\sigma}_2 \cdot \left(\tilde{\mathbf{p}} - \frac{\mathbf{k}}{2} \right) \times \boldsymbol{\epsilon}_\gamma \right] \right\} + (1 \leftrightarrow 2), \end{aligned} \quad (\text{A.7})$$

$$\begin{aligned} \mathcal{O}_h = & \frac{eg_A}{16Mf_\pi^3} \frac{\boldsymbol{\sigma}_1 \cdot (\tilde{\mathbf{p}} + \frac{\mathbf{k}}{2})}{(\tilde{\mathbf{p}} + \frac{\mathbf{k}}{2})^2 + m_\pi^2} \left[(\epsilon^{abc} \tau_1^b \tau_2^c - \epsilon^{a3b} \tau_1^b) \boldsymbol{\epsilon}_\gamma \cdot \tilde{\mathbf{p}} \right. \\ & \left. + \left(\delta^{a3} \boldsymbol{\tau}_1 \cdot \boldsymbol{\tau}_2 - \tau_1^3 \tau_2^a \right) [(1 + \kappa_1) \boldsymbol{\sigma}_2 \cdot (\boldsymbol{\epsilon}_\gamma \times \mathbf{k}) - i2\mathbf{P} \cdot \boldsymbol{\epsilon}_\gamma] \right] + (1 \leftrightarrow 2). \end{aligned} \quad (\text{A.8})$$

3. Double-propagator diagrams

The momentum-space expressions for the third row of diagrams in Fig. 1 are

$$\mathcal{O}_i = 0, \quad (\text{A.9})$$

$$\begin{aligned} \mathcal{O}_j = & \frac{eg_A}{8Mf_\pi^3} \frac{\boldsymbol{\epsilon}_\gamma \cdot \tilde{\mathbf{p}} \boldsymbol{\sigma}_1 \cdot (\tilde{\mathbf{p}} + \frac{\mathbf{k}}{2})}{(\tilde{\mathbf{p}} - \frac{\mathbf{k}}{2})^2 [(\tilde{\mathbf{p}} + \frac{\mathbf{k}}{2})^2 + m_\pi^2]} \left[-8\epsilon^{a3b} \tau_1^b \left(4\hat{c}_1 - 2\hat{c}_2 - 2\hat{c}_3 + \frac{g_A^2}{4} \right) m_\pi^2 \right. \\ & \left. + i \left(\delta^{a3} \boldsymbol{\tau}_1 \cdot \boldsymbol{\tau}_2 - \tau_1^a \tau_2^3 \right) \left(2\mathbf{P} + \frac{\mathbf{k}}{2} \right) \cdot \left(\tilde{\mathbf{p}} - \frac{\mathbf{k}}{2} \right) \right] + (1 \leftrightarrow 2), \end{aligned} \quad (\text{A.10})$$

$$\begin{aligned} \mathcal{O}_k = & \frac{eg_A^3}{4Mf_\pi^3} \frac{\boldsymbol{\epsilon}_\gamma \cdot \tilde{\mathbf{p}} \boldsymbol{\sigma}_1 \cdot (\tilde{\mathbf{p}} + \frac{\mathbf{k}}{2})}{(\tilde{\mathbf{p}} - \frac{\mathbf{k}}{2})^2 [(\tilde{\mathbf{p}} + \frac{\mathbf{k}}{2})^2 + m_\pi^2]} \left\{ \epsilon^{a3b} \tau_1^b \left[\left(\tilde{\mathbf{p}} - \frac{\mathbf{k}}{2} \right)^2 \right. \right. \\ & \left. \left. + i\boldsymbol{\sigma}_2 \cdot \left(2\mathbf{P} + \frac{\mathbf{k}}{2} \right) \times \left(\tilde{\mathbf{p}} - \frac{\mathbf{k}}{2} \right) \right] \right. \\ & \left. - i \left(\delta^{a3} \boldsymbol{\tau}_1 \cdot \boldsymbol{\tau}_2 - \tau_1^a \tau_2^3 \right) \left(2\mathbf{P} + \frac{\mathbf{k}}{2} \right) \cdot \left(\tilde{\mathbf{p}} - \frac{\mathbf{k}}{2} \right) \right\} + (1 \leftrightarrow 2). \end{aligned} \quad (\text{A.11})$$

4. Contact term

The contact term that contributes to ${}^3S_1 \leftrightarrow {}^1S_0$ transitions at $\mathcal{O}(Q^4)$ is given by

$$\begin{aligned} \mathcal{O}_{\text{CT}} = & \frac{eg_A}{Mf_\pi^3} \left[\left(\hat{d}_1 + \frac{\hat{c}_3}{3} - \frac{g_A^2}{12} \right) \epsilon^{a3b} (\tau_1^b \boldsymbol{\sigma}_1 \cdot \boldsymbol{\epsilon}_\gamma + \tau_2^b \boldsymbol{\sigma}_2 \cdot \boldsymbol{\epsilon}_\gamma) \right. \\ & \left. + \left(\hat{d}_2 + \frac{\hat{c}_4}{3} + \frac{1}{12} - \frac{g_A^2}{24} \right) (\tau_1^a \tau_2^3 - \tau_1^3 \tau_2^a) \boldsymbol{\epsilon}_\gamma \cdot (\boldsymbol{\sigma}_1 \times \boldsymbol{\sigma}_2) \right]. \end{aligned} \quad (\text{A.12})$$

Obviously, this contact term can not contribute to processes involving a neutral pion. When put into a ${}^1S_0 \rightarrow {}^3S_1$ matrix element, specialized to $\pi^- d \rightarrow nn\gamma$ (or rather $\gamma nn \rightarrow d\pi^-$), and summed over nucleon spins and isospins, this operator reduces to

$$\frac{2ieg_A}{Mf_\pi^3} \left(\hat{d} - \frac{g_A^2}{6} \right) \boldsymbol{\epsilon}_d^\dagger \cdot \boldsymbol{\epsilon}_\gamma, \quad (\text{A.13})$$

where \hat{d} is given by Eq. (4). The g_A^2 term is the extra piece coming from diagrams (c), (g), and (k).

-
- [1] S. R. Beane, C. Y. Lee, and U. van Kolck, Phys. Rev. C **52**, 2914 (1995); S. R. Beane, V. Bernard, T.-S. H. Lee, U.-G. Meißner, and U. van Kolck, Nucl. Phys. **A618**, 381 (1997).
 - [2] H. Krebs, V. Bernard, and U.-G. Meißner, Nucl. Phys. A **713**, 405 (2003); Eur. Phys. J. A **22**, 503 (2004).
 - [3] V. Bernard, N. Kaiser, and U.-G. Meißner, Nucl. Phys. A **607**, 379 (1996); H. W. Fearing, T. R. Hemmert, R. Lewis, and C. Unkmeir, Phys. Rev. C **62**, 054006 (2000); V. Bernard, N. Kaiser, and U.-G. Meißner, Eur. Phys. J. A **11**, 209 (2001).
 - [4] V. Bernard, N. Kaiser, and U.-G. Meißner, Phys. Lett. B **382**, 19 (1996).
 - [5] V. Lensky *et al.*, Eur. Phys. J. A **26**, 107 (2005).
 - [6] A. Gårdestig and D. R. Phillips, Phys. Rev. C **73**, 014002 (2006).
 - [7] A. Gårdestig and D. R. Phillips, [arXiv.org/abs/nucl-th/0603045].
 - [8] R. Machleidt and I. Slaus, J. Phys. G: Nucl. and Part. Phys. **27**, R69 (2001).
 - [9] V. Bernard, N. Kaiser, and U.-G. Meißner, Int. J. Mod. Phys. E **4**, 193 (1995).
 - [10] V. Bernard and Ulf-G. Meißner, private communication.
 - [11] T.-S. Park *et al.*, Phys. Rev. C **67**, 055206 (2003).
 - [12] T. D. Cohen, J. L. Friar, G. A. Miller, and U. van Kolck, Phys. Rev. C **53**, 2661 (1996).
 - [13] Nadia Fettes, Ulf-G. Meißner, and Sven Steininger, Nucl. Phys. A **640**, 199 (1998).
 - [14] S. Ando *et al.*, Phys. Lett. B **555**, 49 (2003).
 - [15] S. Ando *et al.*, Phys. Lett. B **533**, 25 (2002).
 - [16] C. Hanhart, U. van Kolck, and G. A. Miller, Phys. Rev. Lett. **85**, 2905 (2000).
 - [17] A. Gårdestig and D. R. Phillips, in progress (2006).
 - [18] B. Mosconi, P. Ricci, and E. Truhlík, Eur. Phys. J. A **25**, 283 (2005); [arXiv.org/abs/nucl-th/0212042].
 - [19] This follows the notation adopted by Cohen *et al.* [12], i.e., these d_i 's should not be confused with the ones used for third order πN scattering [13].